터널과 지하공간, 한국암반공학회
Vol. 10, 2000, pp. 447~456

TUNNEL & UNDERGROUND Vol. 10, 2000, pp. 447-456
J. of Korean Society for Rock Mech.

Rock bridges를 고려한 수치 해석적 수압파쇄 균열거동 연구

최 성 웅[1)]

A Numerical Study of Hydraulic Fractures Propagation with Rock Bridges

Sung-Oong Choi

ABSTRACT Rock bridge in rock masses can be considered as one of several types of opening-mode fractures, and also it has been known to have a great influence on the stability of structures in rock mass. In the beginning of researching a rock bridge it used to be studied only in characteristics of its behavior, as considering resistance of material itself. However the distribution pattern of rock bridges, which can affect the stability of rock structures, is currently researched with a fracture mechanical approach in numerical studies. For investigating the effect of rock bridges on the development pattern of hydraulic fractures, the author analyzed numerically the stress state transition in rock bridges and their phenomena with a different pattern of the rock bridge distributions. From the numerical studies, a two-crack configuration could be defined to be representative of the most critical conditions for rock bridges, only when cracks are systematic and same in their length and angle. Moreover, coalescence stresses and onset of propagation stresses could be known to increase with decreasing ***s/L*** ratio or increasing ***d/L*** ratio. The effect of pre-existing crack on hydraulic fracturing was studied also in numerical models. Different to the simple hydraulic fracturing modeling in which the fractures propagated exactly parallel to the maximum remote stress, the hydraulic fractures with pre-existing cracks did not propagate parallel to the maximum remote stress direction. These are representative of the tendency to change the hydraulic fractures direction because of the existence of pre-existing crack. Therefore ***s/L***, ***d/L*** ratios will be identical as a function effective on hydraulic fractures propagation, that is, the K_I value increase with decreasing ***s/L*** ratio or increasing ***d/L*** ratio and its magnification from onset to propagation increases with decreasing ***s/L*** ratio. The scanline is a commonly used method to estimate the fracture distribution on outcrops. The data obtained from the scanline method can be applied to the evaluation of stress field in rock mass.

Key words : rock bridges, opening-mode fracture, hydraulic fractures, stress intensity factor

초 록 : 일반적으로 암반 구조물의 안정성에 심각한 영향을 미칠 수 있는 것으로 알려진, 암반 내의 rock bridges는 일종의 opening-mode fracture로 간주될 수 있다. 초창기에는 재료의 저항 특성을 고려하여 rock bridges 자체의 거동 특성에 대한 연구가 있었으나, 최근에 와서는 수치 해석적 연구를 통해 파괴역학의 개념을 적용하여 rock bridges의 분포특성이 암반 구조물의 안정성에 미치는 영향 등을 새롭게 연구하고 있다. 본 연구에서는 rock bridges가 수압파쇄 균열의 분포특성에 미치는 영향을 규명하고자, rock bridges의 분포형태에 따른 암반 내 응력 분포 특성과 균열의 bridge 현상을 먼저 살펴보았다. 즉, 균열의 길이에 대한 균열의 간격의 비(s/L 비)와 균열의 길이에 대한 균열의 오버랩의 비(d/L 비)를 변화시키면서 응력 분포 특성을 수치 해석적으로 살펴본 결과, 2개의 균열만으로도 여러 개의 균열 분포 특성을 대표할 수 있음을 알았고, s/L 비가 감소할수록 또는 d/L 비가 증가할수록 암반 내 응력 집중은 커짐을 알 수 있었다. 이러한 수치 해석결과를 토대로, 수압파쇄 균열과 rock bridges의 상호 관계를 수치 해석적으로 연구한 결과, rock bridges가 없을 경우 탄성이론에 맞게 발전하던 수압파쇄 균열이, rock bridges의 존재에 의해 수압파쇄 균열의 전파 방향이 왜곡됨은 물론 수압파쇄 균열에 수직으로 작용하는 원거리 응력도 정확히 표현하지 못함을 알았다. 즉, 수압파쇄 균열 선단에서의 mode I 응력집중계수는 s/L 비가 감소할수록 또는 d/L 비가 증가할수록 커짐을 알 수 있었다. 이러한 연구결과로부터, 균열의 분포특성을 규명하기 위해 노두에서 일반적으로 실시되는 scanline 조사에서 얻을 수 있는 s/L 비와 d/L 비를 통하여 암반 내에 존재하는 응력의 평가 방법이 새로이 제안될 수 있을 것이다.

핵심어 : rock bridges, opening-mode fracture, 수압파쇄균열, 응력집중계수

1)정회원, 한국자원연구소 탐사개발연구부 선임연구원
원고접수일 : 2000년 7월 31일
원고 심사 완료일 : 2000년 8월 22일

1. INTRODUCTION

The opening-mode fractures are commonly found in sedimentary rocks. One is called "unconfied" and the other is called "confined". Because the length of the unconfined fractures is much smaller than the layer thickness, and the confined fractures often are confined to a particular layer and terminate at the layer boundaries. Pollard and Aydin (1988) have analyzed that opening-mode fractures in rock are composed of two opposing surfaces that originally were bonded together to form an intact rock mass. The shape of a two-dimensional opening-mode fracture subject to uniform loading in a homogeneous material is an ellipse, theoretically. For that reason, the orientation of an opening-mode fracture that is favored energetically is with the minor axis parallel to the remote maximum tensile stress (Pollard and Segall, 1987). Especially the aperture of opening-mode fractures has been studied basically because fracture aperture and fracture aspect ratio can be used to estimate the fracture driving stress, the fracture accommodated strain and even the fracture toughness of the surrounding rock (Segall and Pollard, 1983). And also opening-mode fractures provide pathways for underground fluid flow (Renshaw and Pollard, 1994). Pollard and Segall (1987) explained also the periodical appearance of joints in layered rocks as a result of the fracture normal stress returning about to its remote value at a certain distance from the original fractures, which is proportional to the layer thickness. Taixu (1998) studied the relation between the fracture spacing and layer thickness with numerical works for opening-mode fractures in layered rocks. According to his conclusions, the normal stress in the direction perpendicular to the fractures changes from tensile to compressive when the fracture spacing/layer thickness ratio goes from greater to smaller than a critical value, which is approximately 1.0.

Rock bridges in non-fully persistent discontinuity sets can be considered as one kind of unconfined fractures which are one of two types of opening-mode fractures. They are known as a significant factor affecting the rock structure stability. Several authors have studied the behavior of rock bridges in itself as well as in relation to rock slope stability (Jennings (1970), Einstein et al. (1983), and Stimpson (1978)). Most of their studies have accomplished by the conventional concepts of the resistance of materials. Recently fracture mechanics concepts have been applied to these phenomena through the numerical methods (Castelli et al. (1997) and Scavia & Castelli (1996)).

In an effort to explain the problem of the behavior of rock bridges as well as opening-mode fractures in compressive stress fields, the author studied the stress state between the adjacent cracks. The author investigated stress as a function of crack spacing/crack length ratio and crack overlapping/crack length ratio. To this end, a series of numerical analyses was carried out in order to simulate the behavior of crack propagation in the uncracked rock mass.

Hydraulic fracturing is a possible mechanism to produce new cracks in rock which has rock bridges. Different to the problem of the stress state only for rock bridges, internal fluid pressure generated by hydraulic fracturing can make a different distribution pattern of stress field in rock mass. Consequently the change of direction of crack propagation can be expected with hydraulic fracturing in rock bridge materials. In the following sections, the FEM results will be introduced and it will be discussed on the implications of the results for the study of crack distribution pattern in rock, which is exposed to the remote compressive stress field as well as internal stress field by fluid pressure.

2. NUMERICAL STUDIES

2.1 Stress state transition on crack configuration

2.1.1 Finite Element Code

We used a two-dimensional finite element code named FRANC2D/L (FRacture ANalysis Code for 2-D Layered structures) to do the numerical modeling work. This code was originally developed at Cornell University and modified for multi-layers at Kansas State University, and is based on the theory of linear and non-linear elastic fracture mechanics (Wawrzynek and Ingraffea, 1987).

Fig. 1(a) shows the conceptual crack growth methodology used in FRANC2D/L (Potyondy, 1993). The general methodology starts with the pre-processing stage, where the geometry, mesh, material properties, and boundary conditions are specified. The result of preprocessing is the initial representation, R_i. The

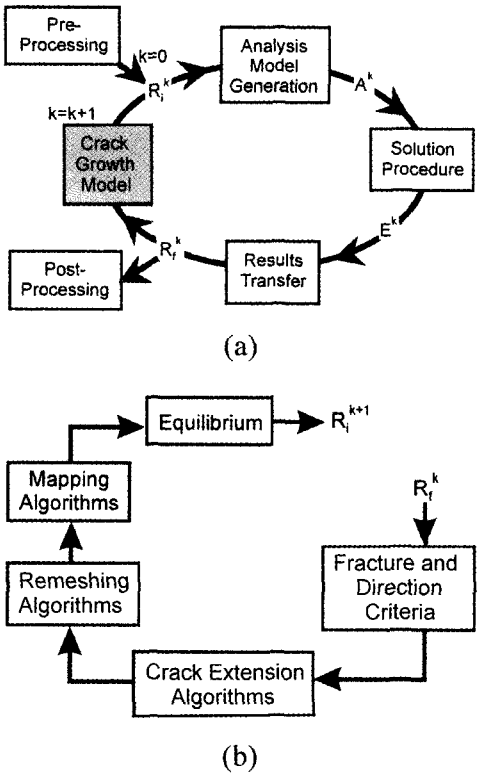

Fig. 1. (a) Conceptual crack growth methodology used in FRANC2D/L (b) and details of Crack Growth Model (Potyondy, 1993 and James, 1998).

Analysis Model Generation phase of the methodology extracts data from the database and converts the data into a form that is efficient for the analysis phase. This phase includes such steps as building a traditional node and connectivity list from the database, optimizing the equation numbering to minimize the stiffness matrix profile, and initializing all of the data structures necessary for the Solution Procedure.

The Solution Procedure is responsible for applying boundary conditions and satisfying the equilibrium equations. The solution procedure is nonlinear incremental-iterative. As the solution progresses, the Solution Procedure is also responsible for monitoring fracture parameters as appropriate times during the analysis, and responsible for initiating appropriate actions when fracture criteria are satisfied.

The output from the Solution Procedure phase is the Results Transfer phase. This step in the methodology transfers the equilibrium output from the solution procedure to the final representation appropriate for post-processing and the crack growth model.

The final step, and the essence of the crack growth methodology, is the Crack Growth Model. Fig. 1(b) focuses in more detail on the Crack Growth Model (James, 1998). The input to the model is R_f^k, the final representation, based on the current equilibrium state. The first step of the Crack Growth Model is to apply the fracture and direction criteria to determine the crack growth direction. In the case of linear fracture mechanics the direction criteria may be dependent upon the fracture criterion, while in the case of elastic-plastic fracture mechanics the direction criterion is more likely to be dependent upon the stress or strain state local to the crack tip, and may or may not be tied to the fracture criterion in a theoretical sense.

The Crack Extension Algorithms grow the crack using the predicted direction and user specified crack growth increment. This step of the methodology first deletes the mesh in the region local to a crack tip, then extends the crack.

The Remeshing Algorithms place a rosette of elements around the crack tip, then rebuild the mesh around the crack tip. The crack extension and remeshing algorithms are essentially the same as for the original LEFM implementation, but modifications transparently manage elastic-plastic related data.

The fourth step of the Crack Growth Model is essential for elastic-plastic crack growth. The Mapping Algorithms are responsible for maintaining the plastic history and displacement solution across the mesh changes created by the crack extension and remeshing algorithms. The plastic history includes primarily nodal displacements and gauss point stresses, but also includes the stress work, radius of the yield surface, and flags that indicate yielding state.

The final step of the Crack Growth Model is to return the model to equilibrium, resulting in a new initial representation model, R_i^k, at the new geometric configuration. Conceptually, this step takes place as part of the crack growth model. For efficiency reasons, during automatic propagation equilibrium is re-established as the initial step of the solution procedure.

2.1.2 Numerical Model

The model and its boundary and loading conditions are shown in Fig. 2. The propagation of cracks slanted

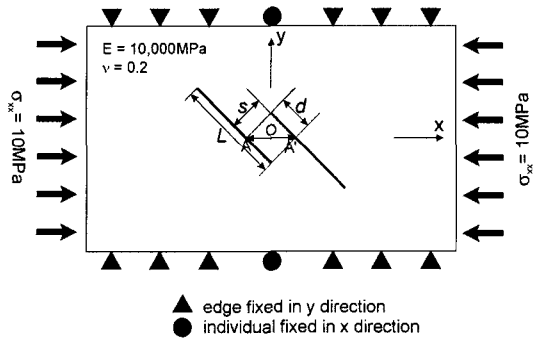

Fig. 2. A numerical model with two-crack configuration (crack length L, crack spacing s and crack overlapping d). The homogeneous material which has 10,000 MPa of Young's modulus and 0.2 of Poisson's ratio is subjected to a remote compressive stress field of 10 MPa.

relative to the vertical and subjected to a horizontal compressive stress in plane strain conditions was analyzed. As shown in Fig. 2, the homogeneous material which has 10,000 MPa of Young's modulus and 0.2 of Poisson's ratio is subjected to a remote compressive stress field of 10 MPa. The 10,000 MPa of Youngs modulus is quite high relative to the in-situ values, but it was for the outstanding figures of rock bridge phenomena. In situ rock masses can not show results exactly same to those in numerical works not because of their quantity of physical properties but because of their heterogeneity.

The configuration of cracks can be also shown in Fig. 2. This configuration is defined by crack length L, crack spacing s and crack overlapping d.

With the assumption of L = 8 m and crack inclination $\alpha = 45°$, a series of analyses was carried out with each case of s/L = 1/4, 1/2, 3/4, and d/L = 0, 1/4, 1/2, 3/4 to evaluate the influence of spacing or overlapping so as to identify a s/L ratio and d/L ratio which are critical for the resistance of the rock bridge. And each case was investigated in both stages of onset of propagation and crack coalescence.

Fig. 3 shows the location of the tensile areas for two extreme overlapping conditions ($s/L = d/L = 1/2$) before the onset of propagation and after crack coalescence. It shows also the fact that the tensile stress areas relative to the two cracks partly coincide and accelerate the propagation of the cracks into the rock bridge. From

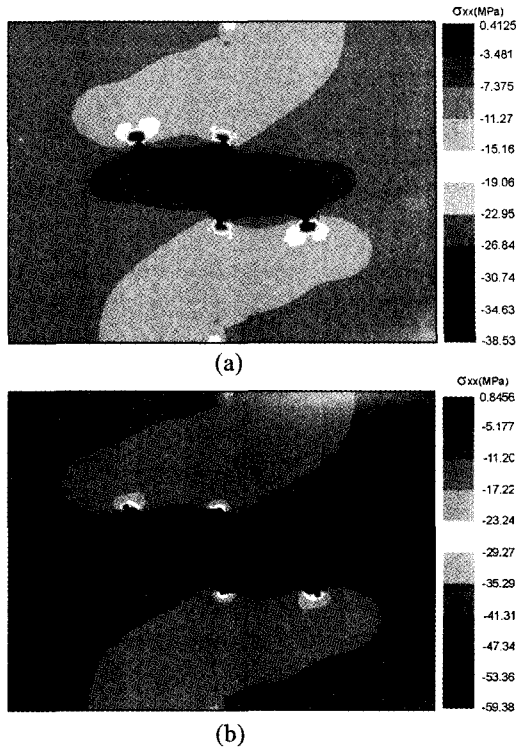

Fig. 3. Tensile stress areas for a two-crack configuration. (a) before the onset of propagation, (b) after crack coalescence. A remote compressive stress is 10 MPa, and $s/L = d/L = 1/2$ in both cases.

patterns of the tensile stress areas in Fig. 3, we can expect that crack spacing/crack length ratio and crack overlapping/crack length ratio will play an important role in facilitating the crack propagation into the rock bridge.

2.1.3 Effects of crack spacing/crack length ratio and crack overlapping/crack length ratio on stress state transition

To show the stress state change as a function of crack spacing/crack length (s/L ratio) and crack overlapping/crack length (d/L ratio), we plot the distribution of σ_{xx}. Fig. 4 shows the distribution patterns of σ_{xx} before the onset of propagation and after crack coalescence along the line AA' in Fig. 2. The s/L ratio is fixed to 1/2 and the d/L ratio varies from 0 to 3/4. From Fig. 4 it can be seen that the propagation is unstable for low values of d/L and becomes stable with increasing d/L. And also for high values of d/L, it can be seen that there are little changes in stress along the line AA' between the onset

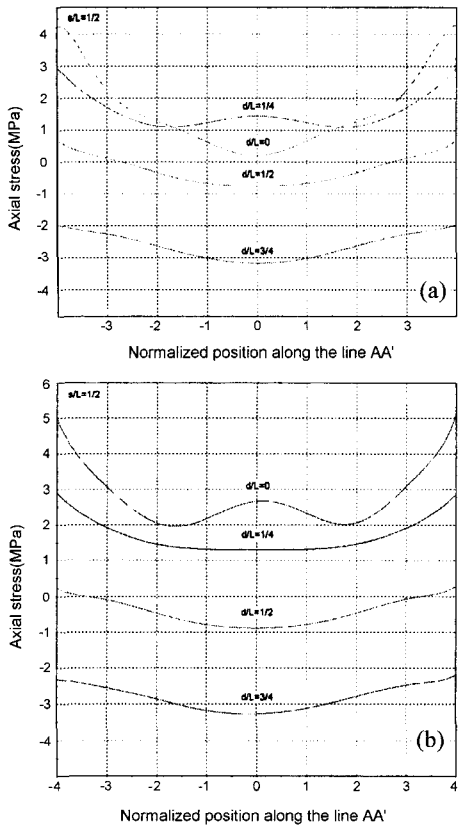

Fig. 4. Distribution patterns of σ_{xx} along the line AA' in Fig. 2 as a function of crack overlapping/crack length ratio (***d/L***) with fixing crack space/crack length ratio (***s/L***) to 1/2. (a) before the onset of propagation, (b) after crack coalescence.

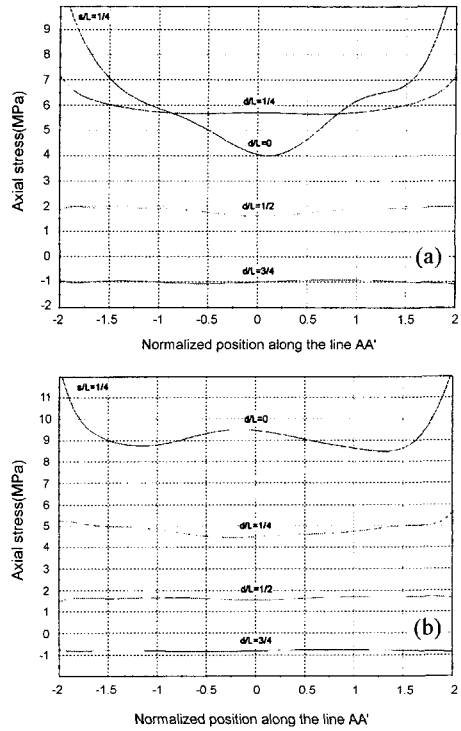

Fig. 5. Distribution patterns of σ_{xx} along the line AA' in Fig. 2 as a function of crack overlapping/crack length ratio (***d/L***) with fixing crack space/crack length ratio (***s/L***) to 1/4. (a) before the onset of propagation, (b) after crack coalescence.

of propagation and crack coalescence, but for low values of ***d/L***(<1/4), the magnitude of axial stresses in the center of the line AA' on the stage of crack coalescence is seemed to be increased by 1.8 times of them on the stage of the onset of propagation.

In order to investigate the effect of ***s/L*** ratio on the distribution patterns of σ_{xx}, the same numerical works were performed with ***s/L*** = 1/4 (Fig. 5) and 3/4 (Fig. 6). The phenomena of the stress distribution with changing ***d/L*** ratio are similar to the case of ***s/L***=1/2 (refer to Fig. 4), but the lower values of ***s/L*** ratio are, the higher values of stress magnitude are shown.

Fig. 6. Distribution patterns of sxx along the line AA' in Fig. 2 as a function of crack overlapping/crack length ratio (***d/L***) with fixing crack space/crack length ratio (***s/L***) to 3/4. (a) Before the onset of propagation, (b) After crack coalescence.

For a better understanding, the stress quantities on the center of the line AA' were plotted according to the ***d/L*** ratio and ***s/L*** ratio in Fig. 7. We can infer from Fig. 7 that coalescence stresses and onset of propagation stresses increase with decreasing ***s/L*** ratio or increasing ***d/L*** ratio. At the same time, propagation is gently stable when ***d/L*** ratio is greater than 0.5. When ***d/L*** ratio is less than 0.25, however, propagation is unstable. In other words, the smaller ***d/L*** ratio is and the the smaller ***s/L*** ratio is, the more unstable propagation is.

2.1.4 Effects of crack amounts on stress state transition

From the foregoing analyses we could identify a two-crack configuration. Now we are going to investigate the effect of crack amounts on the tensile stress field in rock bridges. For this work, a three-, a four- and a five-crack configuration were analyzed separately with a fixed ratio of ***s/L*** = 1/4, ***d/L*** = 1/2 (Fig. 8). From the results of

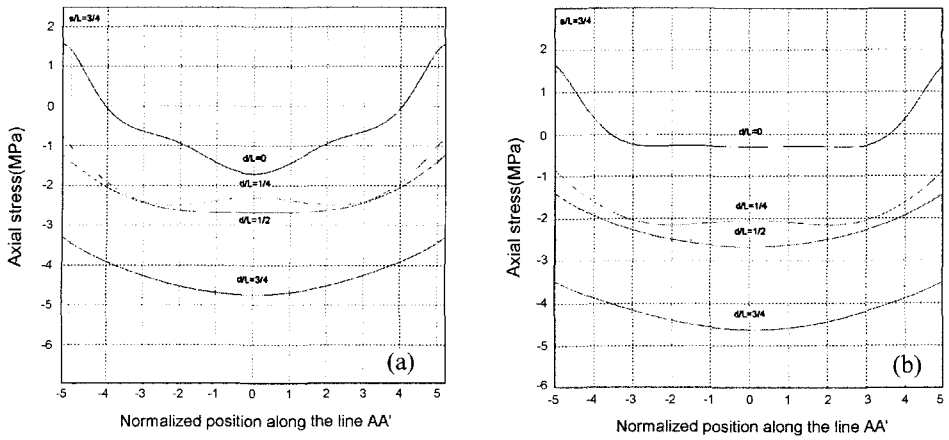

Fig. 6. Distribution patterns of σ_{xx} along the line AA' in Fig. 2 as a function of crack overlapping/crack length ratio (***d/L***) with fixing crack space/crack length ratio (***s/L***) to 3/4. (a) before the onset of propagation, (b) after crack coalescence.

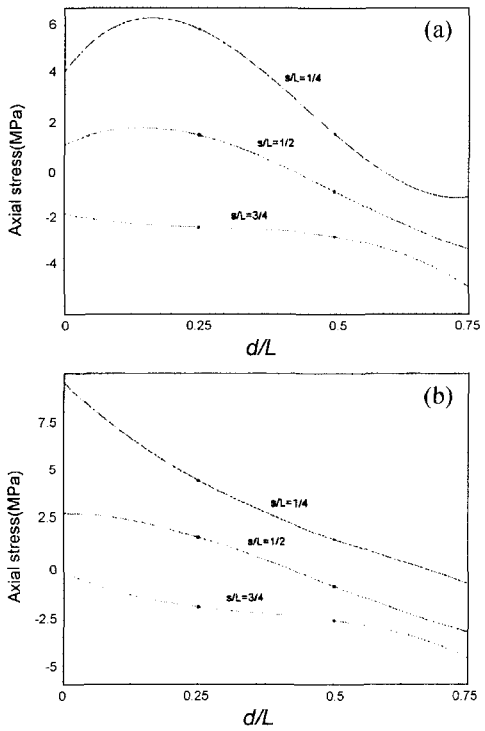

Fig. 7. Axial stress plot with ***s/L*** ratio and ***d/L*** ratio. (a) For onset of propagation, (b) for crack coalescence.

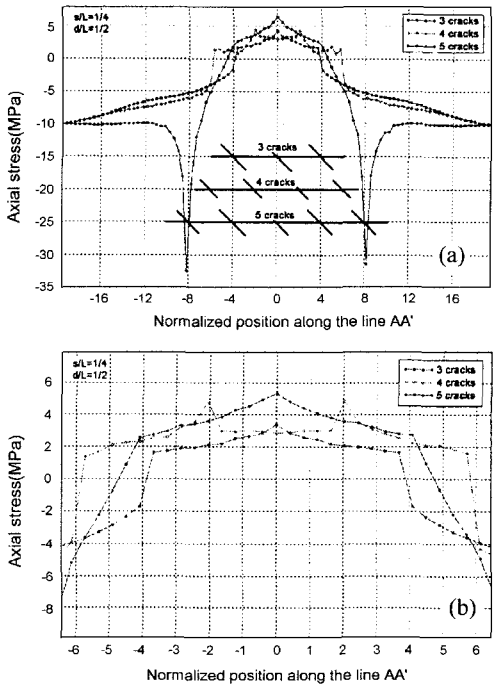

Fig. 8. Distribution patterns of σ_{xx} along the line AA' on several cases of crack quantity with fixing ratio of ***d/L*** = 1/2, ***s/L*** = 1/4. (a) before the onset of propagation for the whole length of model, (b) after crack coalescence for the x-range of crack location only.

Fig. 8, however, we are able to expect that the amount of crack does not play an important role in the critical conditions for rock bridges. The jumps in axial stress shown in Fig. 8(a) for 5 cracks are related only to the existence of cracks. Therefore we can conclude that a two-crack configuration is representative of the most critical conditions for rock bridges.

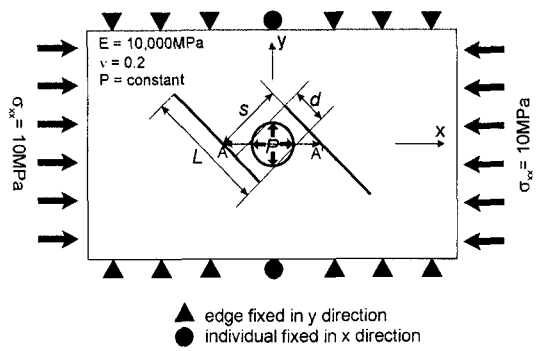

Fig. 9. A numerical model with two-crack configuration and internal pressurized hole (Boundary and loading conditions are same to those of Fig. 2 with notations for crack).

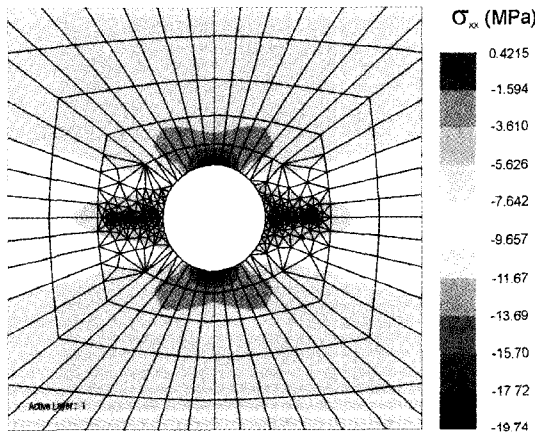

Fig. 10. Stress state transition in hydraulic fracture propagation. Tensile stress areas are shown along the hydraulic fractures which develop parallel to the direction of σ_{xx} with the length equal to the radius of the internal hole.

2.2 Stress state transition on hydraulic fracturing with pre-existing cracks

2.2.1 Numerical Model

From the foregoing analyses we have verified the effects of rock bridges on stress state transition in rock. In hydraulic fracturing field, a large number of methods are provided for a better evaluating the in-situ stress regime. At the early period, rock mass was considered to be homogenous, isotropic and impermeable. But more complicated approaches including fracture mechanics are recently introduced not only for a massive rock mass but also for a jointed rock mass.

In this section, the author would like to show the stress state transition during hydraulic fracturing in rock mass which has rock bridges. Crack configuration is expected to affect the hydraulic fracture propagation not only in their length but also in their direction.

To show the stress state transition on hydraulic fracturing in rock mass with cracks, we used a same two-dimensional finite element model as in Fig. 2 except that they have an internal pressure hole in the center of model (Fig. 9).

2.2.2 Effects of pre-existing crack on hydraulic fracturing

In order to show the coupling effect of pre-existing crack on hydraulic fracturing, we considered, at first, a simple hydraulic fracturing without any cracks. As shown in Fig. 10, the new cracks are developed hydraulically from the right and the left edge of internal hole to the direction parallel to σ_{xx}. Even though the length of crack developed is not important in our numerical models, we are able to know that the crack length equals to the radius of internal hole when the internal pressure is fixed to 10 MPa. Thereafter, the internal pressure will be fixed at a constant value of 10 MPa through the whole numerical models and it will not play a role as a function. And also we can know that the stresses generated in upper and lower edge of internal hole are about 20 MPa and this value shows elastically the summation of the compressive stress concentrated at these areas by the remote stress and the tensile stress by internal pressure.

Now we are trying to investigate the effect of pre-existing cracks on hydraulic fracture propagation. We are able to consider a hole intersected by a pre-existing crack. This should be modeled by a one-crack configuration. The pre-existing crack slanted relative to the vertical and subjected to a horizontal compressive stress in plain strain conditions passes through the center of the internal hole. Fig. 11(a) shows the stress state transition after the development of new hydraulic fractures in a one-crack configuration. The direction of hydraulic fractures is not exactly parallel to the maximum remote stress and the stress normal to hydraulic fracture faces does not coincide with the minimum remote stress, that is, 0 MPa. In Fig. 10 where there is no pre-existing crack, the normal stress to hydraulic fracture faces was almost 0. Moreover, hydraulic fracturing in a one-crack configuration makes a high

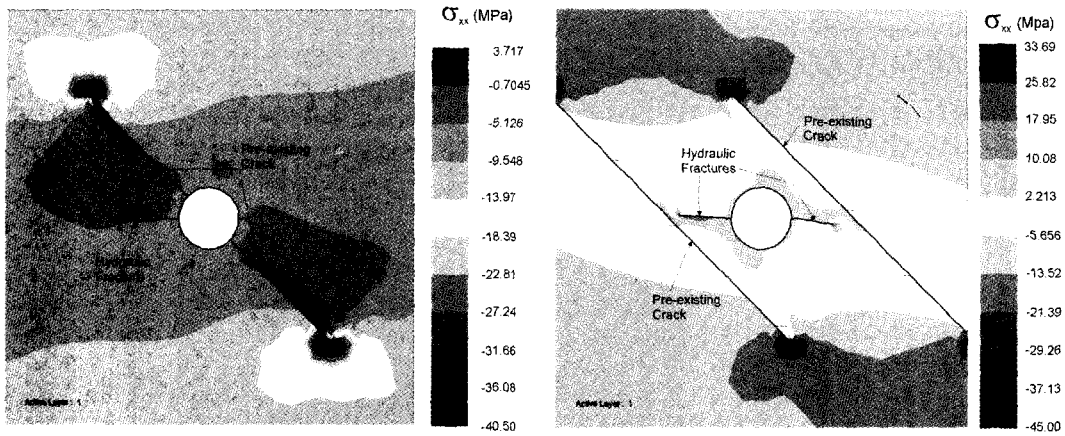

Fig. 11. Stress state transition after hydraulic fracture propagation. (a) One-crack configuration, (b) two-crack configuration. We can see the new-developed hydraulic fracture as well as the propagation of pre-existing crack, and the direction of hydraulic fractures is not exactly parallel to the direction of σ_{xx}.

stress concentration in pre-existing crack tips. From the contour of stress in Fig. 11, we could know that the instantaneous shut-in pressure after stopping the internal pressure cannot stand for the minimum remote stress perpendicular to the crack face.

For more general field cases, we need to a series of pre-existing crack in numerical model. In this section, however, we are going to consider only a two-crack configuration (Fig. 11(b)) because a two-crack configuration was proved to be representative of the most critical conditions for rock bridges in section 2.1. But we need to pay attention to a two-crack configuration in simulations of a hydraulic fracturing. Because a two-crack configuration could be proved to be representative of the most critical conditions only when cracks have same lengths and same angles. Different long and non-parallel cracks should be investigated later.

The numerical results in Fig. 11(b) are very similar to those of Fig. 11(a) in the propagation direction of hydraulic fractures. Especially a two-crack configuration, as shown in Fig. 11(b), shows a possibility of connecting the pre-existing crack to hydraulic fractures. This phenomenon means that the hydraulic fractures tend to change their direction because of the existence of pre-existing crack. Therefore crack space/crack length ratio and crack overlapping/crack length ratio will be identical as a function effective on hydraulic fractures propagation.

As same to the foregoing modeling, the stress state transition and the hydraulic fracture propagation were investigated with a different ***s/L*** ratio and a different ***d/L*** ratio. There will be several factors that should be studied in detail for each numerical case. But in this paper we consider only the mode I stress intensity factor (K_I) in hydraulic crack tips with its length developed. Because the length or curvature of hydraulic fractures can be different with a different ***s/L*** and ***d/L*** ratio and K_t is a critical value for linear elastic fracture mechanical approaches for hydraulic fracturing (Rummel, 1987), e.g.;

$$K_I(S_H,\ S_h,\ P_W,\ P_a) = K_I(S_H) + K_I(S_h) + K_I(P_W) + K_I(P_a) \quad (1)$$

$$K_I(S_H) = -(S_H)\ (r)^{1/2}\ f(b) \quad (2)$$

$$K_I(S_h) = -(S_h)\ (r)^{1/2}\ g(b) \quad (3)$$

$$K_I(P_W) = P_W\ (r)^{1/2}\ h(b) \quad (4)$$

$$K_I(P_a) = P_a\ (r)^{1/2}\ i(b) \quad (5)$$

where, K_I is the stress intensity factor for mode I crack propagation, S_H and S_h are the maximum and minimum remote horizontal stresses, P_W is internal borehole pressure and P_a is the pressure inside the fracture. And f, g, h, i are dimensionless stress intensity functions with $b = 1 + a/r$ (a is a half of crack length and r is a radius of internal hole).

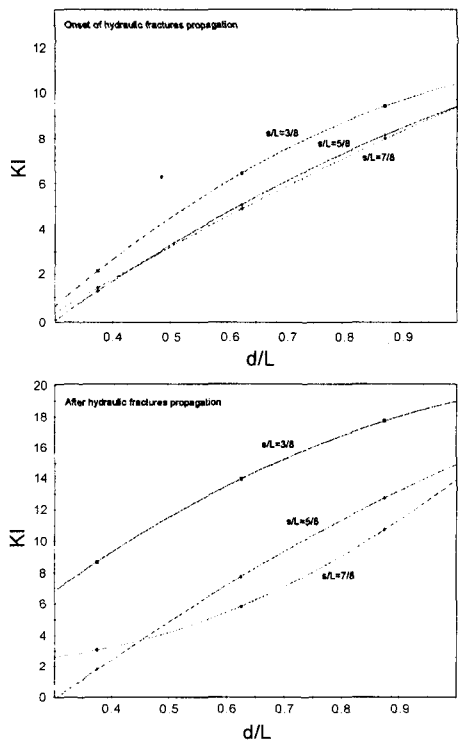

Fig. 12. A mode I stress intensity factor plot with ***s/L*** ratio and ***d/L*** ratio (Unit of K_I is MPa $\sqrt{m}$). (a) For onset of hydraulic fractures propagation, (b) after hydraulic fractures propagation.

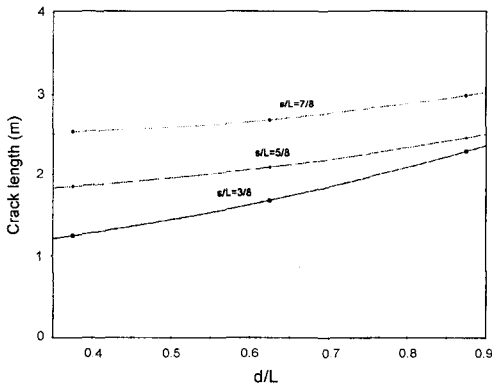

Fig. 13. A crack length plot with **s/L** ratio and **d/L** ratio.

In our cases, it will be fine for us to specify only the $K_I(P_a)$ because every parameter except for a crack length is fixed constant.

Fig. 12(a) and (b) show K_I values which are just prior to beginning of hydraulic fractures and after its propagation, respectively, with a different ***s/L*** and ***d/L*** ratio. From these figures, we can realize that the K_I value increase with decreasing ***s/L*** ratio or increasing ***d/L*** ratio, not only in case of onset of hydraulic fractures propagation but also in case of terminated fractures propagation. This phenomenon is very similar to the former numerical works on stress state transition with rock bridge. And also we can be immediately aware that a magnification of the stress intensity factor from onset to propagation increases with decreasing ***s/L*** ratio.

Finally a length of cracks developed hydraulically can be plotted with a different ***s/L*** and ***d/L*** ratio, as shown in Fig. 13. Contrary to the stress intensity factor plot, crack length increases with increasing s/L ratio and d/L ratio.

3. CONCLUSIONS

From a numerical study of the stress state transition in rock bridges, we could define that a two-crack configuration is representative of the most critical conditions for rock bridges when cracks are systematic, that is, same in their length and angle. And the ***s/L***, ***d/L*** ratio could be proved to play an important role in distribution of tensile stress field. Namely, coalescence stresses and onset of propagation stresses increase with decreasing ***s/L*** ratio or increasing ***d/L*** ratio.

To show the effect of pre-existing crack on hydraulic fracturing, we considered a simple hydraulic fracturing without any cracks, a hydraulic fracturing in a one-crack configuration, and a hydraulic fracturing in a two-crack configuration with a series of ***s/L***, ***d/L*** ratios. Different to the simple hydraulic fracturing modeling in which the fractures propagated exactly parallel to the maximum remote stress, the hydraulic fractures with pre-existing cracks did not propagate parallel to the maximum remote stress direction. These are representative of the tendency to change the hydraulic fractures direction because of the existence of pre-existing crack. Therefore ***s/L***, ***d/L*** ratios will be identical as a function effective on hydraulic fractures propagation. From the plots of the stress intensity factor for mode I crack propagation, it was interpreted that the K_I value increase with decreasing ***s/L*** ratio or increasing ***d/L*** ratio and its magnification from onset to propagation increases with decreasing ***s/L*** ratio. And from the plots of crack length, we could know that crack length increases with

increasing ***s/L*** ratio and ***d/L*** ratio.

The scanline is a commonly used method to estimate the fracture distribution on outcrops. The data obtained from the scanline method can be applied to the evaluation of stress field in rock mass. For more accurate analysis, several factors such as the pre-existing crack angle, the pre-existing crack persistency, the differentials of the remote stresses, and the variation of internal pressure should be studied in the future.

ACKNOWLEDGEMENTS

This research has been supported by the Korea Science and Engineering Foundation. I would like to thank David D. Pollard for his helpful advice and suggestions.

REFERENCES

1. Amadei, B. and O. Stephansson, 1997, Rock stress and its measurement, Chapman & Hall, 121-199.
2. Castelli, M., M. Cravero, G. Iabichino and C. Scavia, 1997, Tensile crack propagation in artificial specimens with two slits, Proc. Int. Symp. on Deformation and Progressive Failure in Geomechanics, IS NAGOYA' 97, 163-168.
3. Einstein, H. H., D. Veneziano, G. B. Baecher and K. J. O'Reilly, 1983, The effect of discontinuity persistence on rock slope stability, Int. J. of Rock Mech. Min. Sci. Geomech. Abstr., 20, 225-236.
4. James, M. A., 1998, A plane stress finite element model for elastic-plastic mode I/II crack growth, Ph.D. Thesis, Dept. Mechanical and Nuclear Engineering, College of Engineering, Kansas State University, Manhattan, Kansas.
5. Jennings, E. B., 1970, A mathematical theory for the calculation of the stability of slopes in open cast mines, Open Pit Mining Symp., Johannesburg, 87-102.
6. Pollard, D. D. and A. Aydin, 1988, Progress in understanding jointing over the past century, Geological Society of America Bulletin, 100, 1181-1204.
7. Pollard, D. D. and P. Segall, 1987, Theoretical displacements and stresses near fractures in rocks: with applications to faults, joints, veins, dikes and solution surfaces, in Atkinson, B. K., eds., Fracture Mechanics of Rock, Academic Press, London, 277-349.
8. Potyondy, D. O., 1993, A software framework for simulating curvilinear crack growth in pressurized thin shells, Ph.D. Thesis, Cornell University, Ithaca, New York.
9. Renshaw, C. E. and D. D. Pollard, 1994, Numerical simulation of fracture set formation: a fracture mechanics model consistent with experimental observations, J. of Geophysical Research, 99, 9359-9372.
10. Rummel, F., 1987, Fracture mechanics approach to hydraulic fracturing stress measurements, in Atkinson, B. K., eds., Fracture Mechanics of Rocks, Academic Press, London, 217-239.
11. Scavia, C. and M. Castelli, 1996, Analysis of the propagation of natural discontinuities in rock bridges, Proc. ISRM Int. Symp. on Prediction and Performance in Rock Mechanics and Rock Engineering, EUROCK' 96, Torino, Italy, 1, 445-451.
12. Scavia, C., 1999, The displacement discontinuity method for the analysis of rock structures: a fracture mechanics approach, , in M. H. Aliabadi eds., Fracture of Rock, WITpress, London, 39-82.
13. Segall, P. and D. Pollard, 1983, Joint formation in granitic rock of Sierra Nevada, Geological Society of America Bulletin, 94, 563-575.
14. Stimpson, B., 1978, Failure of slopes containing discontinuous planar joints, Proc. 19th U.S. Symp. On Rock Mechanics, Nevada University, 296-300.
15. Taixu, B., 1998, Spacing of opening-mode fractures in layered rocks, Proc. of the Rock Fracture Project in Stanford University, 9, P-A.
16. Wawrzynek, P. A. and A. R. Ingraffea, 1987, Interactive finite element analysis of fracture processes: An integrated approach: Theoretical and Applied Fracture Mechanics, 8, 137-150.

최 성 웅

1987년 서울대학교 공과대학 자원공학과, 공학사
1989년 서울대학교 대학원 자원공학과, 공학석사
1994년 서울대학교 대학원 자원공학과, 공학박사

Tel : 042-868-3243
E-mail : choiso@kigam.re.kr
choiso@pangea.stanford.EDU
현재 한국자원연구소 탐사개발연구부 선임연구원
Visiting Researcher, Rock Fracture Project Group, Stanford University